Topological Disposition of Cys 222 in the α-Subunit of Nicotinic Acetylcholine Receptor Analyzed by Fluorescence-Quenching and Electron Paramagnetic Resonance Measurements†

Jeongah Kim and Mark G. McNamee*

Section of Molecular and Cellular Biology, University of California, Davis, California 95616

Received October 27, 1997; Revised Manuscript Received January 23, 1998

ABSTRACT: The structure of the nicotinic acetylcholine receptor (AChR) has been studied using a combination of fluorescence quenching and electron paramagnetic resonance (EPR) collision gradient methods. The AChR from *Torpedo californica* was labeled with a fluorescent probe, *N*-(1-pyrenyl)-maleimide, specific for sulfhydryls in a hydrophobic environment, under conditions of selective labeling of Cys222 in the α-subunit. αCys222 is located in the postulated M1 transmembrane domain and predicted to be at the center of an α-helical secondary structure. The spatial disposition of the acetylcholine receptor-bound pyrene with respect to the membrane bilayer was assessed by fluorescence quenching measurements. Quenching of pyrene fluorescence by spin-labeled fatty acids with the doxyl group at positions C-5 and C-12 revealed that the former was more effective, suggesting that the fluorophore is located closer to the membrane−water interface than to the hydrophobic interior. Power saturation EPR spectroscopy was also used to examine the effect of molecular oxygen and water-soluble paramagnetic reagents on the saturation behavior of a nitroxide spin label, which was specifically attached to the same αCys222 residue. Using the gradients of these paramagnetic reagents through the membrane−solution interface, the distance for the nitroxide derivative from the membrane−solution interface was measured to be approximately 7 Å from the headgroup region of the phospholipid bilayer, in agreement with fluorescence quenching results. These results suggest that the M1 transmembrane domain of the AChR probably forms an irregular structure, a β-strand, or an α-helical structure that may span the membrane in a way different from a linear α-helix.

The nicotinic acetylcholine receptor (AChR)[1] is a member of a family of ligand-gated ion channels, which includes the serotonin receptor ($5HT_3$), the glycine receptor, and the $GABA_A$ receptor (see review in refs *1*−*4*). The function of AChR is to recognize and specifically bind the neurotransmitter acetylcholine released from a nerve ending. The AChR converts the chemical signal into an electric signal consisting of a depolarization of the postsynaptic membrane triggered by the flux of cations through the receptor's ion channel.

The nicotinic AChR from *Torpedo californica* electric organ is a heterologous asymmetric protein composed of five polypeptide chains of four different subunit types. The resulting quaternary structure is α_2, β, γ, and δ. These polypeptide chains have molecular masses M_r of 40 (α), 48 (β), 60 (γ), and 68 kDa (δ), and the polypeptide chains are glycosylated. cDNA cloning and complete sequencing of the AChR subunits from *T. californica* has been carried out (*5*, *6*). Hydropathy profiles suggest that each subunit contains four transmembrane crossings which are denoted as M1, M2, M3, and M4, and nearly all models suggest an α-helical transmembrane secondary structure.

Over the past several years, application of molecular and electrophysiological techniques have greatly expanded the knowledge of the muscle-type AChRs and the closely related neuronal AChRs. In most neuronal tissues, the AChR is composed of only one or two distinct subunits believed to be arranged in a pentameric structure with a stoichiometry $(\alpha)_5$ or $(\alpha)_2(\beta)_3$ (*7*, *8*). These receptors are present on autonomic neurons and adrenal chromaffin cells in the peripheral nervous system and on many neurons in the central nervous system (reviewed in refs *9* and *10*). From rat and chick, at least eight α-subunits (α2−α9) and three β-subunits (β2−β4) have been cloned (*11*, *12*). The α2−α9-subunits are presumed to contain the primary binding site for acetylcholine while the β-subunits are structurally analogous to *Torpedo* β, γ, and δ subunits.

† This research was supported by a research grant to M.G.M. from National Institutes of Health (NS22941) and a Jastro-Shields graduate research scholarship to J.K.

* Corresponding author: Division of Biological Sciences, University of California, Davis, CA 95616. Phone: (530) 752-6764. Fax: (530) 752-2604. E-mail: mgmcnamee@ucdavis.edu.

[1] Abbreviations: AChR, nicotinic acetylcholine receptor; Carb, carbamylcholine; CHS, cholesterol hemisuccinate; DOPA, dioleoylphosphatidic acid; DOPC, dioleoylphosphatidylcholine; 5-DXPC, 5-doxyl dioleoylphosphatidylcholine; 12-DXPC, 12-doxyl dioleoylphosphatidyl choline; 5-DXSA, 5-fatty acid spin label (5-doxylstearic acid); 12-DXSA, 12-fatty acid spin label (12-doxylstearic acid); EDTA, ethylenediamine tetraacetic acid; EPR, electron paramagnetic resonance; [^{125}I]BgTx, [^{125}I]iodinated α-bungarotoxin; MOPS, 3-(*N*-morpholino)-propanesulfonic acid; MTS-SL, *S*-(1-oxy-2,2,5,5-tetramethylpyrrolin-3-yl-3-methyl)methane thiosulfonate spin-label; NiEDDA, nickel ethylenediamine-*N*,*N*′-diacetic acid; NPM, *N*-(1-pyrenyl)maleimide; SDS, sodium dodecyl sulfate; [^{125}I]TID, 3-(trifluoromethyl)-3-(*m*-[^{125}I]-iodophenyl)diazirine.

S0006-2960(97)02666-4 CCC: $15.00
Published on Web 03/11/1998

A high-resolution structure of AChR is not available because of the difficulty inherent in crystallizing hydrophobic membrane proteins. Therefore, development of alternative methods for obtaining structural information is important. Recently, images of AChR in the absence and in the presence of acetylcholine have been obtained by electron microscopy at a resolution of 9 Å using giant tubular membrane arrays prepared from isolated *Torpedo* postsynaptic membranes (*13*−*15*). A single kinked rod of high density is seen in the transmembrane domain of each subunit and is hypothesized to be an α-helix that lines the narrow portion of the channel. On the basis of other evidence that the M2 segments line the channel (*16*−*18*), Unwin postulated that the kinked rod was the M2 segment and concluded that the other membrane-spanning segments (M1, M3, and M4) form β-strands and that the membrane-embedded β strands from all five subunits together form a large β-barrel surrounding the five α-helical M2 segments. This view is contrary to the original assumption that all the membrane-spanning segments are entirely α-helical (*5*, *6*).

In contrast to the ultrastructural studies, the labeling patterns obtained from hydrophobic photoaffinity probes suggest an α-helical periodicity in the exposure of both M3 and M4 to the hydrophobic core of the lipid bilayer (*19*, *20*). The labeling of M1 is consistent with an α-helix that is slightly distorted due to the presence of a proline residue in the C-terminal half of the hydrophobic region (*20*). Recently, cysteine mutagenesis combined with covalent chemical modification of cysteines that face the channel indicated that the first half of M1 is nonhelical (*21*).

We report here the use of two different approaches to examine the secondary structure of the putative first transmembrane domain, M1, which is highly conserved among the four AChR subunits and across all species, including invertebrates (see review in refs *9* and *22*). The αCys222 residue is invariant among vertebrate AChRs and is replaced by Ser or Thr in several invertebrate AChR subunits, in the $GABA_A$ β subunit, and in glycine receptors. Since αCys222 is positioned at the middle of the primary sequence of the M1 transmembrane domain (Figure 1), it can be located at very different regions of the lipid bilayer depending on the secondary structure and the subsequent folding pattern of M1. In this paper, we investigate the location of the αCys222 residue in the membrane to determine which secondary structures of M1 are compatible with the experimental results. First, we labeled Cys222 in the α-subunit with *N*-(1-pyrenyl)maleimide, a fluorescent probe specific for sulfhydryls in a hydrophobic environment. Spin-labeled fatty acids and phospholipids were used to cause a differential quenching of the cysteine-bound pyrenes (*23*). Second, the αCys222 was selectively labeled with a small, sulfhydryl-specific reagent, methanethiosulfonate nitroxide spin label (MTS-SL). The accessibility of the spin-labeled residue to lipid-soluble molecular oxygen and to the lipid-impermeable nickel−EDDA complexes was measured from the saturation properties of the electron paramagnetic resonance (EPR) spectra (*24*).

MATERIALS AND METHODS

Materials. Cholesterol hemisuccinate (CHS), *N*-(1-pyrenyl)maleimide (NPM), and fatty acid spin labels were purchased from Sigma (St. Louis, MO). *S*-(1-Oxy-2,2,5,5-tetramethylpyrrolinyl-3-methyl)methane thiosulfonate (MTS-SL) was from Reanal Factory of Laboratory Chemicals, Hungary. Chloroform solutions of all synthetic phospholipids were obtained from Avanti Polar Lipids (Birmingham, AL). Ultrol grade sodium cholate of very high purity was from Calbiochem (San Diego, CA). Affigel-10 was from Bio-Rad. [^{125}I]Iodinated α-bungarotoxin ([^{125}I]BgTx, >200 μCi/mmol) was obtained from Amersham (Arlington Heights, IL). *Staphylococcus aureus* V8 protease and proteinase K were from ICN Biochemical Corporation. Molecular weight standards were from Gibco/BRL (Gaithersburg, MD). Other chemicals used were of reagent grade.

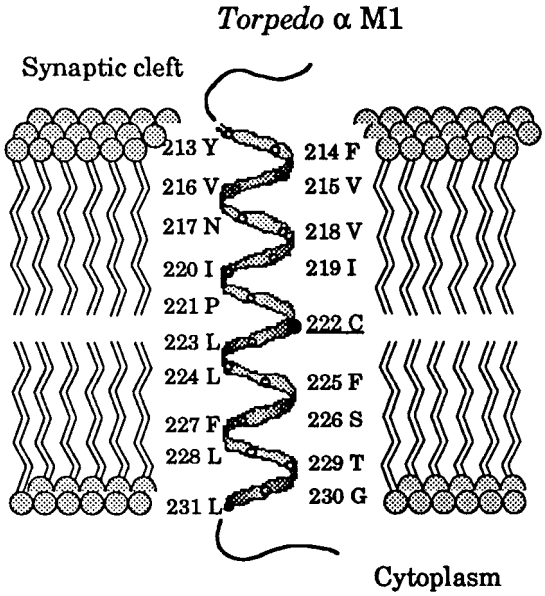

FIGURE 1: Helical representation of the M1 transmembrane domain of the *Torpedo* nAChR α-subunit.

Purification of Acetylcholine Receptor. The acetylcholine receptor was purified on an affinity column from crude membrane preparations of the frozen electroplax tissue from *T. californica* using dioleoylphosphatidylcholine (DOPC) as the added lipid during purification (*25*, *26*). AChR purity was established by SDS−gel electrophoresis. The purified receptor was dialyzed for 48 h against three changes of buffer A (10 mM MOPS, 0.1 mM EDTA, 100 mM NaCl, and 0.02% NaN_3, pH 7.4) and had a lipid-to-protein ratio of about 400−500:1. The protein concentrations were determined by the Lowry method (*27*), and the lipid concentration was determined by measuring the lipid phosphate content (*28*).

Labeling of Receptor with NPM and MTS-SL and the Reconstitution with Lipids. For fluorescence and EPR studies involving AChR in reconstituted lipids, purified AChR was prepared in DOPC at a lipid-to-protein ratio of 400−500:1 and prelabeled with 1 mM *N*-1-ethylmaleimide (NEM) in the presence of 1% cholate. The reaction mixture was incubated under nitrogen for 5 min on ice, and unbound NEM was removed by dialyzing the mixture against buffer A for 2 days at 4 °C with three buffer changes. NEM-prelabeled AChR was treated with 1 mM NPM in the presence of 1% cholate for 1.5 h at room temperature. For the MTS-spin labeling, a concentrated stock solution of MTS-SL in acetonitrile was introduced into the NEM-prelabeled membrane solution in buffer A. The samples were incubated at 20 °C for 2 h. Labeled AChRs were loaded back onto

the affinity column previously equilibrated with 1% cholate to remove all unbound labels. The receptor was washed extensively with buffer A containing DOPC and cholate, eluted by the addition of carbamylcholine, and then reconstituted in DOPC:DOPA:CHS (60:20:20) to a final lipid-to-protein ratio of 1000:1.

Enzymatic Digestion of Labeled AChR and Gel Electrophoresis. NPM or MTS-SL labeled proteins were separated by SDS−PAGE on 11 cm long, 3.0 mm thick 8% polyacrylamide gels. The NPM-labeled subunits were visualized by examining the gels on a UV transilluminator. Incorporation of MTS-SL on proteins was confirmed by detecting the nitroxide spin signal of each subunit, which was isolated from excised gel pieces using passive elution (*29*). Once α-subunit specific fluorescence or spin labeling on AChR was confirmed by preparative SDS−PAGE, the α subunit fragments containing labeled polypeptides were transferred to the wells of individual 15% tricine-SDS−polyacrylamide mapping gels (*20, 30*). Tricine gels were composed of a 8 cm long separating gel (15% T/6% C), 3 cm long spacer gel (10% T/3% C), and 2 cm long stacking gel (4% T/3% C) as described before (*31*). Each well containing excised α subunit fragments was overlaid with sample loading buffer containing 50 μg of *Staphylococcus aureus* V8 protease. Electrophoresis was carried out at 20 mA for about 15 h. Direct visualization using UV light was performed to identify the band containing fluorescent NPM residues on the mapping gels. MTS-spin-labeled peptide bands were identified by EPR measurements following the isolation of four major bands from mapping gels and concentration of each peptide solution using Amicon Centricon-3 concentrator.

To confirm that labeling by MTS-SL and NPM occurred in the transmembrane portion of AChR, water-exposed AChR regions were removed by treatment with proteinase K as described (*32*). After 24 h of incubation of the protease with labeled AChR, the samples were centrifuged at 100000*g* for 30 min, and the resulting pellet and supernatant were separated. After the lyophilization of supernatants and washing of pellets with buffer A, both supernatants and pellets were subjected to EPR and fluorescence emission spectrum measurements to follow their signals.

Determination of Toxin Binding Sites on AChR. Equilibrium binding of [^{125}I]BgTx to AChR in Triton X-100 was measured by trapping negatively charged AChR−toxin complexes on DEAE (DE81) filters, according to Fong and McNamee (*33*), with one modification. DE81 filters were placed in Packard Pony Vials, 4 mL of CytoScint liquid scintillation fluid added, and the filters were incubated overnight at room temperature. The vials were then counted for 1 min on a Packard Tri-Carb 1500 Liquid Scintillation Analyzer set for iodine-125.

Rate of Toxin Binding Assays. The rates of [^{125}I]BgTx binding were measured in the absence of detergent, as described by Sunshine and McNamee (*34*). Three different types of binding rate constants were determined at 20 °C: (1) k_{max}, the pseudo-first-order rate constant in the absence of Carb; (2) k_{co}, the pseudo-first-order rate constant when 10 mM Carb was added at the same time as toxin; and (3) k_{pre}, the pseudo-first-order rate constant determined after exposure of the receptor proteins to 10 mM Carb for 30−60 min at 20 °C. For each toxin binding reaction, samples were taken at 30, 60, 90, 120, 150 s, and 1 h and filtered through DE81 filters. The filters were treated and counted as described above.

Fluorescence Intensity Measurements. Steady-state fluorescence measurements were performed on an SLM 8000C spectrofluorometer (SLM Instruments, Urbana, IL) operating in the ratio mode with a 1-cm-path-length quartz cuvette. For intensity measurements, 0.04−0.05 μM pyrene-labeled AChR in DOPC:DOPA:CHS was diluted in 1 mL of buffer A as described before (*23*). The spin-labeled fatty acids at the indicated concentrations, ranging from 0 to 8 μM, were added directly to the above and incubated at room temperature for 30 min before fluorescence measurements to ensure incorporation of probes. Excitation and emission wavelengths for the pyrene residues were 345 and 376 nm, respectively; slit widths were 4 nm for both wavelengths. The sample absorbance was always <0.1, thereby eliminating inner filter effects and light scattering. All internal correction was made automatically for changes in lamp intensity by using a reference solution of rhodamine B (3 g/L) in ethylene glycol. All measurements were performed at room temperature. Collisional quenching theory and parameters are the same as those described in earlier works (*35, 23*).

EPR Spectroscopy. EPR spectra of labeled AChR were recorded using a Bruker ESP300 spectrometer equipped with a loop gap resonator (Medical Advances Inc., Milwaukee, WI) and a low-noise amplifier (Miteq, Hauppauge, NY). Spin-labeled proteins were dissolved in buffer A to the desired concentration, and the resulting solution was thoroughly mixed by vortexing and allowed to stand for 30 min before EPR measurements.

Immersion Depth Measurements. The immersion depths of the nitroxide spin labels were measured by the EPR collision gradient method developed by Altenbach et al. (*24*). The depth measurements were performed using spin-labeled AChR solutions in a gas-permeable TPX capillary to allow saturation of the samples with air or nitrogen. The EPR spectra at 0.1, 0.25, 1, 4, 8, 10, 16, 25, and 40 mW incident microwave power were measured, and the peak-to-peak amplitudes of the first derivative $M_I = 0$ EPR lines were used to obtain the saturation profiles in the presence of membrane permeable molecular oxygen and membrane impermeable nickel complex paramagnetic relaxants. The measurements were performed and analyzed using a calibration curve based on measurements of spin-labeled bacteriorhodopsins as described previously (*24, 36*).

RESULTS

Labeling AChR by N-(1-Pyrenyl)maleimide. For the selective labeling of the α subunit of AChR at a specific cysteine residue, purified AChR was prelabeled with NEM to block easily labeled sulfhydryl groups, such as Cys416, Cys420, and Cys451 in the γ-subunit (*23, 37, 38*). SDS−PAGE of NEM-prelabeled, NPM-labeled receptor clearly shows under a UV illuminator that the band corresponding to the α subunit in the Coomassie-stained gel is predominantly labeled (Figure 2).

Quenching of NPM-Labeled AChR Fluorescence by Spin-Labeled Fatty Acids and Phospholipids. The spatial relationship of AChR-bound pyrene with respect to the membrane bilayer was studied by fluorescence-quenching measurements. Spin-labeled fatty acids (*23, 39*) and phos-

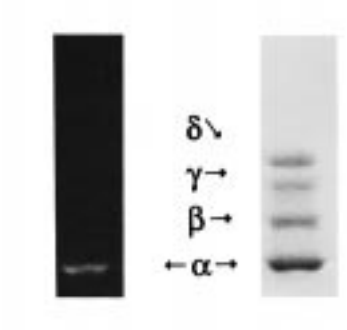

FIGURE 2: SDS−PAGE of the pyrene-labeled AChR subunits on an 8% gel. The left lane shows the fluorogram of the labeled gel as viewed on an UV illuminator. The right lane is the Coomassie stained gel showing the four subunits in the stoichiometry of $\alpha_2\beta\gamma\delta$. Both lanes contained 20 μg of membrane protein.

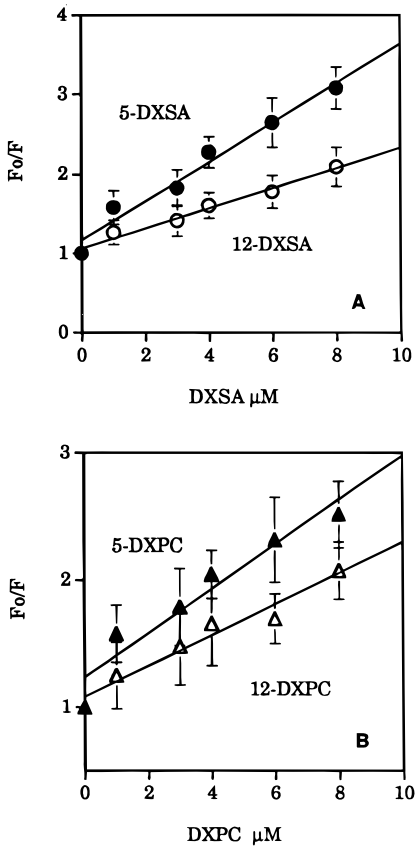

FIGURE 3: Stern−Volmer plot of F_o/F vs concentration of 5- (●, △) and 12- (○, △) spin labeled fatty acids (A) and phosphatidylcholines (B). F_o and F are fluorescence intensities of AChR-bound pyrene in the absence and in the presence of different concentrations of quenchers, respectively. The pyrene labeled AChR concentration was 0.4 μM. The fluorescence emission was measured at 376 nm at an excitation wavelength of 345 nm. The results represent the average of three independent experiments with duplicates from each.

pholipids (*40*) with the doxyl group at different positions along the fatty acyl chain have been successfully used as molecular rulers to locate the depth of membrane-embedded fluorophores.

Spin-labeled stearic acids with the nitroxide group at the C-5 and C-12 positions (5-DXSA and 12-DXSA, respectively) were used to quench the extrinsic fluorescence of pyrene-labeled AChR, and the quenching profiles are shown in Figure 3A. The decrease in fluorescence intensity at 376 nm (when excited at 345 nm) was monitored as a function of increasing concentration of spin-labeled stearic acids. The intensity of unlabeled receptor was used as a reference and subtracted suitably, and the intensity of the pyrene-labeled receptor in the absence of added quencher served as the control, F_o. The 5-DXSA quenched more effectively than the 12-DXSA, indicating a more superficial location for cysteine-bound fluorophores in the α subunit of AChR. The apparent Stern−Volmer quenching constants are shown in Table 1. It is clear that the fluorophores are more easily accessible to 5-DXSA, which has a quenching constant of 0.247, than to 12-DXSA with a quenching constant of 0.128. Similar results were obtained for spin-labeled phospholipid as a quencher in Figure 3B. The apparent quenching constants were 0.174 for 5-DXPC and 0.122 for 12-DXPC, respectively. These values are lower than those for DXSAs, which may be caused by less efficient partitioning of phospholipids compared to fatty acids into the AChR-containing membranes.

Table 1: Apparent Stern−Volmer Quenching Constants for Quenching of αCys222 Pyrene-Labeled AChR Fluorescence by Spin-Labeled Fatty Acids and Phosphatidylcholines

quencher	K_{sv}[a]
5-DXSA	0.237 ± 0.015
12-DXSA	0.128 ± 0.019
5-DXPC	0.174 ± 0.011
12-DXPC	0.122 ± 0.008

[a] Apparent Stern−Volmer quenching constants, K_{sv} from Stern−Volmer plots, Figure 3. Values are averages of ±SEM from three independent experiments with duplicates from each.

Labeling AChR by MTS-Spin Label. To examine the incorporation sites of MTS-SL into reconstituted AChR membranes, a series of SDS−PAGEs and EPR signal measurements were performed. Following MTS-spin labeling of NEM prelabeled AChR, the distribution of labeled AChR among the subunits was carried out using 8% SDS−PAGE. Unlike the pyrene-attached proteins, the spin-labeled subunit(s) cannot be visualized under UV illumination. Therefore, each subunit was purified using passive elution from excised bands and subjected to EPR spin label intensity measurements. The only EPR spectrum strong enough to be identified came from the α subunit, confirming the α subunit specific MTS-spin labeling on the AChR. Considering the stoichiometry of α subunit compared to other subunits, only half the amount of eluted α subunit was used for EPR measurements.

For the mapping of MTS-SL-labeled sites of the AChR α subunit in greater detail, V8 protease was used to digest the protein. Limited digestion of AChR α subunit has been shown to reproducibly generate four well-characterized fragments that run on a 15% SDS−polyacrylamide gel with apparent molecular weights of 20 000 (V8−20), 18 000 (V8−18), 10 000 (V8−10), and 4000 (V8−4) (*30*, *19*). The four principal cleavage products were evident in the Coomassie Blue stained α subunit mapping gel from our experiment (Figure 4). To identify the positions of spin label in the primary structure of the α subunit, these fractionated peptides were purified by passive elution and subjected to EPR measurements. Only the V8−20 fragment showed any spin label signal, suggesting the specific incorporation of MTS-SL into a specific domain of the α subunit region known to contain M1, M2, and M3 (*19*). Since there is only

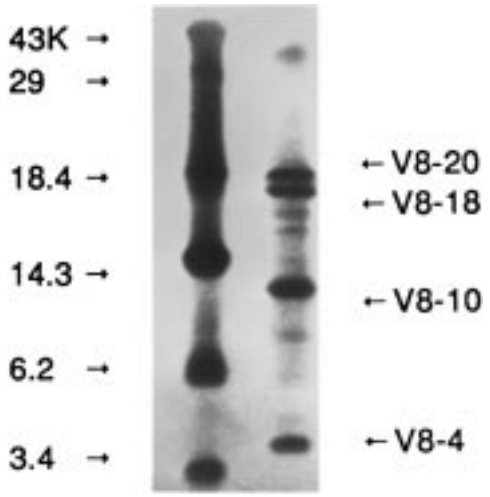

FIGURE 4: Proteolytic mapping of the sites of MTS-SL incorporation on the AChR α-subunit using *S. aureus* V8 protease. AChR-rich membranes containing 380 μg of protein were spin-labeled with MTS and subjected to SDS−PAGE on an 8% slab gel, and the α subunit band excised. The excised band was transferred to the well of a 15% mapping gel and overlaid with 50 μg of *S. aureus* V8 protease. Following electrophoresis, the mapping gel was stained with Coomassie Blue. Migration of the molecular weight markers is indicated on the left for ovalbumin (43K), carbonic anhydrase (29K), β-lactoglobulin (18.4K), lysozyme (14.3K), bovine trypsin inhibitor (6.2K), and the α-chain of insulin (3.4K).

Table 2: Pseudo-First Order [^{125}I]BgTx Binding Rate Constants for Spin-Labeled, NPM-Labeled, and Unlabeled AChR Membranes ($\times 10^3$ s^{-1})[a]

sample	k_{max}[b]	k_{co}	k_{pre}
unlabeled AChR	3.41 ± 0.24	2.08 ± 0.20	0.99 ± 0.05
spin-labeled AChR	3.02 ± 0.54	2.24 ± 0.31	0.82 ± 0.10
NPM-labeled AChR	2.76 ± 0.31	1.88 ± 0.22	0.75 ± 0.06

[a] Pseudo-first-order rate constants were determined from the slope of plots of −ln[1 − cpm(t)/cpm(eq)] vs time (seconds) as detailed in the Materials and Methods. [b] The results are mean of triplicate determinations ± standard deviation.

one free cysteine residue (αCys222) in the V8−20 polypeptide, αCys222 is highly likely to be the residue responsible for selective MTS-SL incorporation into AChR.

For further verification of incorporation sites of fluorophore and spin label into AChR, proteinase K was used to separate the water-exposed AChR regions from its transmembrane domain (*32*). Only the membrane-spanning moieties for both labeling cases showed the positive signals under fluorescence or spin signal measurements. The results are consistent with labeling patterns shown in SDS−PAGEs that αCys222 was the specific site for our chemical modifications.

Rates of Toxin Binding Assays for AChR Membranes. Table 2 lists the values of calculated pseudo-first-order rate constants for [^{125}I]BgTx binding to native and chemically modified AChRs. The difference in rates observed between samples preincubated and coincubated with carbamylcholine is due to the ligand-induced desensitization of the receptor, a key aspect of AChR function. Neither pyrene nor MTS-spin labeling introduced any significant functional changes compared to native membranes. These results support the idea that our chemical modifications have very little or no effect on the native structure of AChR, assuming that a substantial fraction of the AChR was labeled. We have tried to quantitate the stoichiometry of pyrene labeling on the AChR using Beer's Law. The measurements of concentrations for both protein and protein-immobilized pyrene revealed that about 65% of the AChR had been successfully modified by pyrene residues. Since there are no radiolabeled analogues available for the probes we have used, we were unable to determine the exact stoichiometry of labeling for either probe.

Table 3: $\Delta P_{1/2}$ and Φ[a] Values for MTS-Spin Labeled AChRs

$\Delta P_{1/2}$(air), mW	10.5 ± 1.0
$\Delta P_{1/2}$(NiEDDA), mW	6.5 ± 0.6
Φ	0.5 ± 0.2

[a] $\Phi = \ln[\Delta P_{1/2}(\text{air})/\Delta P_{1/2}(\text{NiEDDA})]$. The final protein concentration was 150 μM, and the phospholipid concentration was 150 mM. The concentration of NiEDDA was 200 mM.

Depth Measurements of Spin-Labeled AChRs Using Power Saturation Electron Paramagnetic Resonance. The immersion depth measurement of the spin label at AChR using the collision gradient method is based on the $\Delta P_{1/2}$ values for the membrane permeable (O_2) and impermeable (NiEDDA) relaxing reagents (*24, 41*). The quantity $\Delta P_{1/2}$ is the difference in $P_{1/2}$ values in the presence and absence of relaxing agent, and $P_{1/2}$ is the power where the first derivative amplitude of the EPR signal is reduced to half of its unsaturated value. Table 3 shows $\Delta P_{1/2}(O_2)$ and $\Delta P_{1/2}$(NiEDDA) values for our spin-labeled AChR. The higher $\Delta P_{1/2}(O_2)$ value compared to $\Delta P_{1/2}$(NiEDDA) confirms that the nitroxide attached to the Cys222 of AChR α-subunit is located in the bilayer region rather than exposed to water. According to the depth calibration experiment with bacteriorhodopsin, Φ, the natural log of the ratio of the $\Delta P_{1/2}$ value for the molecular oxygen [$\Delta P_{1/2}(O_2)$] to that for the metal ion complex [$\Delta P_{1/2}$(NiEDDA)], is linearly proportional to the immersion depth (*24*). The Φ value was 0.5 for the MTS-spin labeled AChR, suggesting that our nitroxide spin-label is buried in the acyl chain region at an average depth of 7 Å, close to the water−membrane interface region rather than embedded in the middle of the lipid bilayer. These results are in good agreement with the data from fluorescence quenching experiments.

The other feature of the EPR spectra for the membrane-bound spin label is the reduced solvent-sensitive hyperfine coupling constant, which is obtained by measuring the peak-to-peak distance (*41*). The coupling constant for MTS spin label in water is 16.1 G. On the other hand, the constants are in the range of 14.8−15.0 G when spin label is completely embedded in lipid bilayer. The hyperfine coupling constant for the spin label attached to AChR was 15.5 G, again implying that the Cys222 of α subunit is embedded near the water exposed region in the AChR membrane.

DISCUSSION

The results from the present investigation offer a refined view of the location of Cys222 in the α subunit of the acetylcholine receptor. We made use of spin-labeled fatty acids and phosphatidylcholines to quench the extrinsic

fluorescence of a pyrene moiety attached to Cys222 of the α-subunit, and we used electron paramagnetic resonance measurements to estimate the immersion depth of a nitroxide spin label, covalently linked to the same cysteine residue on the α subunit.

Under our labeling conditions, the α subunit was labeled with either pyrene or the methanethiosulfonate nitroxide spin label, with negligible labeling of the other subunits. Previously, Marquez et al. (*42*) used the same pyrene probe to label the AChR in the native membrane environment in the absence of cholate and concluded that only one of seven Cys residues in the α subunit exists as a free SH, most likely αCys222 on the M1 segment. While two pairs, αCys128−αCys142 and αCys192−αCys193, are located in the synaptic region as disulfide bridges, it is thought that the third pair, αCys412−αCys418, in the M4 segment either may be involved in a thioester linkage or is acylated and does not exist as free sulfhydryls or disulfides (*43*). Protelolytic mapping of the nitroxide-labeled AChR using *S. aureus* protease or proteinase K, followed by spin signal measurements, strongly suggests that Cys222 is the single residue involved in our spin labeling on the α subunit of the AChR.

A major concern in using extrinsic probes is a possible perturbation of protein structure and function by the labels. However, the relatively small size of each probe suggests to us that these probes do not affect AChR membrane integrity. Since we have only measured the vertical depth of probes, not the side-to-side interactions of probes with neighboring residues, it is very unlikely that our probes can cause a major structural disturbance, such as a vertical shift of Cys222 residue in the αM1 segment. The toxin binding rate data provide no evidence for functional perturbation.

Previously, we have made use of spin-labeled fatty acids to quench pyrene residues covalently attached to Cys451 in the γ-subunit of AChR and energy transfer measurements to evaluate the distance between γTrp453 and γCys451 in the AChR (*23*). In the present study, with specific labeling of the αCys222 residue, the fluorescence quenching data suggest that the vertical depth of the pyrene on αCys222 is closer to 6 Å than to 15 Å from the headgroup interface in accordance with the higher level of quenching by 5-DXSA and 5-DXPC. The penetration depth for the doxyl group is assumed to be about 6 and 15 Å for 5- and 12-DXSA, respectively, from the headgroup interface (*44*).

Recently, the collision gradient method for depth measurement of spin label in lipid bilayer was applied to determine the secondary structure of bacteriorhodopsin (*24*). In this method, two fast-relaxing paramagnetic species with finite but different solubilities in the bilayer were used to locate the nitroxide spin labels attached to the protein. Using this experimental strategy, we observed that the MTS-spin label selectively linked to αCys222 of the AChR was located approximately 7 Å from the lipid headgroup region close to the water−lipid interface.

Taking both the fluorescence quenching and electron paramagnetic resonance measurements together, the Cys222 residue in the α-subunit of the AChR is located near the lipid headgroup region. The secondary structure of the M1 segment of the AChR α subunit is likely to be a β-sheet or an irregular structure. Another possibility is that this segment forms an α-helical structure with several short helices connected by turns. A classical α-helical secondary structure would place the αCys222 at the center of the bilayer.

Our results complement the data by Blanton and Cohen (*20*) obtained using a series of hydrophobic, nonspecific labels to lend support to the view that M2, M3, and M4 are helical. They found that M1, M3 and M4 were labeled with [^{125}I]TID and concluded that the labeling patterns were compatible with a helical conformation for M3 and M4. They could not, however, clearly assign the pattern obtained for M1 to an α-helix or a β-sheet. Moreover, the loop connecting M2 and M3, a region not usually considered to be in the membrane, was also labeled.

The all-helical four-transmembrane model has been also questioned on the basis of high-resolution electron microscopy (*13, 14*). In the tubular crystal images of *Torpedo* membranes, only one rod representing an α-helix (presumably M2) was visible in the transmembrane part of each subunit. FT-IR spectroscopy of membrane-bound receptor, from which the extramembrane domains have been removed by proteolysis, detected more than 40% β-structure (*32*). Furthermore, modeling studies showed that a bundle of 5 × 4 transmembrane helices is not compatible with the calculated dimensions of the AChR (*45, 46*). Cysteine mutants investigated by accessibility of Cys residues to thiosulfonate cations show that the secondary structure of the extracellular half of M1 is irregular (*21, 47*).

Several integral membrane proteins, for which the structures have been solved, span the membrane via α-helices (*48*−*50*), but exceptions, most notably the β-barrel structures for porins, are known (*51*). However, no mixed α-helical and β-structure domains have been discovered yet.

It has been reported that mutations made at the Cys230 residue in the γ-subunit altered the energy barrier for a single closing rate constant in proportion to the size of the substituted side chain (*52*). However, those substitutions, when made in the Cys222 in the α subunit, had no effect on gating. These results suggest that M1 segment may not be exposed in the channel. According to Unwin (*13, 15*), the only differences between the closed and open states in the transmembrane regions are at the level of M2s. In the future, our pyrene and spin-labeled αCys222 AChR membrane can be used to determine the structural changes of M1 during its exposure to agonists and antagonists.

ACKNOWLEDGMENT

We thank Drs. T. Thorgeirsson and Y. -K. Shin, Department of Chemistry, University of California, Berkeley, for assisting with electron paramagnetic resonance measurements and helpful suggestions.

REFERENCES

1. Hucho, F., Tsetlin, V. I., and Machold, J. (1996) *Eur. J. Biochem. 239*, 539−557.
2. Karlin, A., and Akabas, M. H. (1995) *Neuron 15*, 1231−1244.
3. Changeux, J.-P. (1995) *Biochem. Soc. Trans. 23*, 195−205.
4. Pradier, L., and McNamee, M. G. (1992) in *The Structure of Biological Membranes* (Yeagle, P. Ed.) pp 1047−1106, Telford, Caldwell, NJ.
5. Noda, M., Takahashi, H., Tanabe, T., Toyosato, M., Kikyotani, S., Furutani, Y., Hirose, T., Takashima, H., Inayama, S., Miyata, T., and Numa, S. (1983) *Nature (London) 302*, 528−532.

6. Claudio, T., Ballivet, M., Patrick. J., and Heinemann, S. (1983) *Proc. Natl. Acad. Sci. U.S.A. 80*, 1111−1115.
7. Cooper, E., Couturier. S., and Ballivet, M. (1991) *Nature 350*, 235−238.
8. Role, L. W., and Berg, D. K. (1996) *Neuron 16* (6), 1077−1085.
9. Lindstrom, J. (1996) *Ion Channels 4*, 377−450.
10. Sargent, P. (1993) *Annu. Rev. Neurosci. 16*, 403−443.
11. Role, L. W. (1992) *Curr. Opin. Neurobiol. 2* (3), 254−262.
12. Gerzanich, V., Anand, R., and Lindstrom, J. (1994) *Mol. Pharmacol. 45*, 212−220.
13. Unwin, N. (1993) *J. Mol. Biol. 229*, 1101−1124.
14. Unwin, N. (1993) *Cell 72 (Suppl.)*, 31−41.
15. Unwin, N. (1995) *Nature 373*, 37−43.
16. Giraudat, J., Dennis, M., Heidmann, T., Hamont, P. Y., Lederer, F., and Changeux, J.-P. (1987) *Biochemistry 26*, 2410−2418.
17. , Villarroel, A., and Sakmann, B. (1992) *Biophy. J. 62*, 196−205.
18. Charnet, P., Labarca, C., Leonard, R. J., Vogelaar, N. J., Czyzyk, L., Gouin, A., Davidson, N., and Lester, H. A. (1990) *Neuron 4*, 87−95.
19. Blanton, M. P., and Cohen, J. B. (1992) *Biochemistry 31*, 3738−3750.
20. Blanton, M. P., and Cohen, J. B. (1994) *Biochemistry 33*, 2859−2872.
21. Akabas, M. H., and Karlin, A. (1995) *Biochemistry 34*, 12496−12500.
22. Claudio, T. (1989) in *In Frontiers in Molecular Biology: Molecular Neurobiology Volume* (Glover, D. M., and Hames, D., Eds.) pp 66−132, Oxford, IRL.
23. Narayanaswami, V., Kim, J., and McNamee, M. G. (1993) *Biochemistry 32*, 12413−12419.
24. Altenbach, C., Greenhalgh, D. A., Khorana, H. G., and Hubbell, W. L. (1994) *Proc. Natl. Acad. Sci. U.S.A. 91*, 1667−1691.
25. Ochoa, E. L. M., Dalziel, A. W., and McNamee, M. G. (1983) *Biochim. Biophys. Acta 727*, 151−162.
26. Bhushan, A., and McNamee, M. G. (1990) *Biochim. Biophys. Acta 1027*, 93−101.
27. Lowry, O. H., Rosebrough, N. J., Farr, A. L., and Randall, R. J. (1951) *J. Biol. Chem. 193*, 265−275.
28. McClare, C. W. F. (1971) *Anal. Biochem. 39*, 527−530.
29. Hager, D. A., and Burgess, R. R. (1980) *Anal. Biochem. 109*, 76−86.
30. White, B. H., and Cohen, J. B. (1988) *Biochemistry 27*, 8741−8751.
31. Schägger, H., and von Jagow, G. (1987) *Anal. Biochem. 166*, 368−379.
32. Görne-Tschelnokow, U., Strecker, A., Kaduk, C., Naumann, D., and Hucho, F. (1994) *EMBO. J. 13*, 338−341.
33. Fong, T. M., and McNamee, M. G. (1986) *Biochemistry 25*, 830−840.
34. Sunshine, C., and McNamee, M. G. (1992) *Biochim. Biophy. Acta 1108*, 240−246.
35. Lakowicz, J. R. (1983) in *Principles of Fluorescence Spectroscopy*, Plenum Press, New York.
36. Thorgeirsson, T. E., Russell, C. J., King, D. S., and Shin, Y.-K. (1996) *Biochemistry 35*, 1803−1809.
37. Narayanaswami, V., and McNamee, M. G. (1993) *Biochemistry 32*, 12420−12427.
38. Li, L., Schuchard, M., Palma, A., Pradier, L., and McNamee, M. G. (1990) *Biochemistry 29*, 5428−5436.
39. Mitra, B., and Hammes, G. G. (1990) *Biochemistry 29*, 9879−9884.
40. Chattopadahyay, A., and McNamee, M. G. (1991) *Biochemistry 29*, 7159−7164.
41. Yu, Y. G., Thorgeirsson, T. E., and Shin, Y.-K. (1994) *Biochemistry 33*, 14221−14226.
42. Marquez, J., Iriarte, A., and Martinez-Carrion, M. (1989) *Biochemistry 28*, 7433−7439.
43. Mosckovitz, R., and Gershoni, J. M. (1988) *J. Biol. Chem. 264*, 10911−10916.
44. Voges, K.-P., Jung, G., and Sawyer, W. H. (1987) *Biochim. Biopys. Acta 896*, 64−76.
45. Ortells, M. O., and Lunt, G. G. (1996) *Protein Eng. 9*, 51−59.
46. Ortells, M. O., Barrantes, G. E., Wood, C., Lunt, G. G., and Barrantes, F. J. (1997) *Protein Eng. 10*, 511−517.
47. Akabas, M. H., Stauffer, D. A., Xu, M., and Karlin, A. (1992) *Science 258*, 307−310.
48. Deisenhofer, J., Epp, O., Miki, K., Huber, R., and Michel, H. (1985) *Nature 318*, 618−624.
49. Henderson, R., Baldwin, J. M., Ceska, T. A., Zemlin, F., Beckmann, E., and Downing, K. H. (1990) *J. Mol. Biol. 213*, 899−929.
50. Pebay-Peyroula, E., Rummel, G., Rosenbusch, J. P., and Landau, E. M. (1997) *Science 277*, 1676−1680.
51. Parker, M. W., Postma, J. P. M., Pattus, F., Tacker, A. D., and Tsernoglu, D. (1992) *J. Mol. Biol. 224*, 639−657.
52. Lo, D. C., Pinkham, J. L., and Stevens, C. F. (1991) *Neuron 6*, 31−40.

BI972666K